

# Elastic $\alpha$ - $^{12}\text{C}$ scattering at low energies in cluster effective field theory

Shung-Ichi Ando<sup>1</sup>,

*School of Mechanical and ICT Convergence Engineering,  
Sunmoon University, Asan, Chungnam 31460, Republic of Korea*

The elastic  $\alpha$ - $^{12}\text{C}$  scattering at low energies is studied employing an effective field theory in which the  $\alpha$  and  $^{12}\text{C}$  states are treated as elementary-like fields. We discuss scales of the theory at stellar energy region that the  $^{12}\text{C}(\alpha, \gamma)^{16}\text{O}$  process occurs, and then obtain an expression of the elastic scattering amplitudes in terms of effective range parameters. Using experimental data of the phase shifts for  $l = 0, 1, 2$  channels at low energies, for which the resonance regions are avoided, we fix values of the parameters and find that the phase shifts at the low energies are well reproduced by using three effective range parameters for each channel. Furthermore, we discuss problems and uncertainties of the present approach when the amplitudes are extrapolated to the stellar energy region.

PACS(s): 11.10.EF, 24.10.-i, 25.55.Ci, 26.20.Fj.

---

<sup>1</sup><mailto:sando@sunmoon.ac.kr>

## 1. Introduction

The radiative alpha capture on carbon-12,  $^{12}\text{C}(\alpha, \gamma)^{16}\text{O}$ , is one of the fundamental reactions in nuclear astrophysics, which determines the ratio  $^{12}\text{C}/^{16}\text{O}$  produced in helium burning [1]. The reaction rate, equivalently the astrophysical  $S$ -factor, of the process at the Gamow peak energy,  $T_G = 0.3$  MeV, however, cannot experimentally be determined due to the Coulomb barrier. It is necessary to employ a theoretical model and extrapolate the cross section down to  $T_G$  by fitting the model parameters to available experimental data measured at a few MeV or larger. During a last half century, a lot of experimental and theoretical studies for the process have been carried out. For reviews, see, e.g., Refs. [2, 3] and references therein.

In constructing a model for the process, one needs to take account of excited states of  $^{16}\text{O}$  [2], particularly, two excited bound states for  $l_{n-th}^\pi = 1_1^-$  and  $2_1^+$  just below the  $\alpha$ - $^{12}\text{C}$  breakup threshold at  $T = -0.045$  and  $-0.24$  MeV<sup>2</sup>, respectively, as well as  $1_2^-$  and  $2_2^+$  resonant (second excited) states at  $T = 2.42$  and  $2.68$  MeV, respectively. Thus the capture reaction to the ground state of  $^{16}\text{O}$  at  $T_G$  is expected to be E1 and E2 transition dominant due to the subthreshold  $1_1^-$  and  $2_1^+$  states. While the resonant  $1_2^-$  and  $2_2^+$  states play a dominant role in the available experimental data at low energies, typically  $1 \leq T \leq 3$  MeV. Experimental data pertaining to processes for nuclear astrophysics are compiled, known as NACRE-II compilation [4], in which the  $S$ -factor of the  $^{12}\text{C}(\alpha, \gamma)^{16}\text{O}$  reaction is estimated employing a potential model and reported uncertainty of the process is less than 20 %. While conflicting sets of experimental data for the process at very low energies still persist [5, 6], and thus one may need to wait for new measurements at very low energies,  $T \leq 1.5$  MeV [3].

In the present study, we would like to discuss an alternative theoretical approach constructing an effective field theory (EFT) for the process, and apply the theory to the study of elastic  $\alpha$ - $^{12}\text{C}$  scattering at low energies. EFTs provide us a model independent and systematic method for theoretical calculations. An EFT for a system in question can be built by introducing a scale which separates relevant degrees of freedom at low energies from irrelevant degrees of freedom at high energies. An effective Lagrangian is written down in terms of the relevant degrees of freedom, and is perturbatively expanded order by order, by counting the number of derivatives. The irrelevant degrees of freedom are integrated out and their effect is embedded in coefficients appearing in the effective Lagrangian. Thus a transition amplitude is systematically calculated by writing down Feynman diagrams, whereas the coefficients appearing in the effective Lagrangian should be determined by experiments. For reviews, one may refer to, e.g., Refs. [7, 8, 9]. Various processes being essential in nuclear astrophysics have been investigated by constructing EFTs, for example,  $p(n, \gamma)d$  at BBN energies [10, 11] and  $pp$  fusion [12, 13, 14, 15] and  $^7\text{Be}(p, \gamma)^7\text{B}$  [16, 17] in the Sun.

An unique feature of those studies in EFTs is that the theories allow us to estimate *theoretical* uncertainties, based on the model-independent and perturbative expansion scheme of the theories, in the extrapolated reaction rates. For example, less than 1 %

---

<sup>2</sup>The energy  $T$  denotes that of the  $\alpha$ - $^{12}\text{C}$  system in center of mass frame.

accuracy in the estimate of the reaction rates of  $p(n, \gamma)d$  at BBN energies and the  $pp$  fusion in the Sun were obtained in the previous studies [11, 14]. Thus our main aim in future studies for the  $^{12}\text{C}(\alpha, \gamma)^{16}\text{O}$  reaction is to estimate the  $S$  factors with about 5 % uncertainty in theory.

We treat the  $\alpha$  and  $^{12}\text{C}$  states as elementary-like fields, and the scales involving in the theory are to be discussed in the next section. Then an effective Lagrangian is written down, an expression of the scattering amplitudes is obtained, and phase shifts for  $l = 0, 1, 2$  channels of the elastic  $\alpha$ - $^{12}\text{C}$  scattering at low energies are studied. The main assumption of the present study, suggested by Teichmann [18], is that we may choose the energies of the resonant states the large energy scale of the theory so that, in the limited low energy regions, the Breit-Wigner type pole structure for the resonant states in the scattering amplitudes can be expanded in terms of the energy and the expression of the energy dependence of the amplitudes can be reduced to that of the effective range expansion. Thus our large energy scales of the theory for the elastic scattering for  $l = 0, 1$ , and 2 channels are the resonance energies,  $T = 4.89, 2.42$ , and 2.68 MeV for the  $0_2^+, 1_2^-, 2_2^+$  states, respectively. In addition, we do not introduce explicate degrees of freedom for the  $1_1^-$  and  $2_1^+$  states. Because, as to be discussed in detail later, the expression of the scattering amplitudes in terms of the effective range parameters have a restrictive condition in zero momentum limit, we find that it is not easy to incorporate the subthreshold states in the present study.

This article is organized in the following. In section 2, we discuss the scales of the theory and write down an effective Lagrangian for the elementary-like  $\alpha$  and  $^{12}\text{C}$  fields. In section 3, the expression of the amplitudes for the elastic  $\alpha$ - $^{12}\text{C}$  scattering for  $l = 0, 1, 2$  channels in terms of the effective range parameters is obtained. In section 4, the parameters are fitted by using the experimental phase shifts, and for a qualitative study of the extrapolation the real part of the denominator of the scattering amplitudes is extrapolated to  $T_G$ . Finally, conclusions and discussion of the present work are presented in section 6.

## 2. Scales and effective Lagrangian for the system

As mentioned above, we treat the  $\alpha$  and  $^{12}\text{C}$  states as elementary-like cluster fields. This treatment would be reasonable when a typical momentum scale is smaller than a scale at which a mechanism at high energy becomes relevant. For the  $\alpha$  particle, excited states of the  $\alpha$  particle should be treated as irrelevant degrees of freedom [19, 20]. First excited energy of the  $\alpha$  particle is  $E_{(4)} \simeq 20$  MeV, and thus a corresponding large momentum scale is  $\Lambda_H \sim \sqrt{2\mu_4 E_{(4)}} \simeq 170$  MeV where  $\mu_4$  is the reduced mass for one and three nucleon systems,  $\mu_4 \simeq \frac{3}{4}m_N$ .  $m_N$  is the nucleon mass. For the  $^{12}\text{C}$  state, on the other hand, first excited energy of  $^{12}\text{C}$  is  $E_{(12)} \simeq 4.439$  MeV, and thus the large momentum scale due to  $E_{(12)}$  is  $\Lambda_H \sim \sqrt{2\mu_{12} E_{(12)}} \simeq 150$  MeV where  $\mu_{12}$  is the reduced mass for four and eight nucleon systems,  $\mu_{12} \simeq \frac{8}{3}m_N$ . In addition, we need to introduce another large scale due to the Coulomb interaction. The inverse of the Bohr radius is  $\kappa = \alpha_E Z_\alpha Z_C \mu \simeq 247$  MeV where  $\alpha_E$  is the fine structure constant,  $Z_\alpha$  and  $Z_C$  are the number of protons in  $\alpha$  and  $^{12}\text{C}$ , respectively, and  $\mu$  is the reduced mass for  $\alpha$  and  $^{12}\text{C}$ ,  $\mu \simeq 3m_N$ . Thus we may choose the large momentum scale of the theory  $\Lambda_H \sim 150$  MeV.

A typical momentum scale  $Q$  for the  $^{12}\text{C}(\alpha,\gamma)^{16}\text{O}$  process in the starts is estimated from the Gamow peak energy,  $T_G \simeq 0.3$  MeV, and thus the typical momentum scale is  $Q \sim k = \sqrt{2\mu T_G} \simeq 41$  MeV. Thus we shall have the expansion parameter for the process at  $T_G$  as  $Q/\Lambda_H \sim 1/3$ , and the about 5 % theoretical uncertainty mentioned above can be achieved by considering perturbative corrections up to next-to-next-to leading order.

A typical momentum scale,  $Q \sim k$ , for the elastic  $\alpha$ - $^{12}\text{C}$  scattering differs from that at  $T_G$ . We employ the phase shift data from Plaga *et al.* [21] and Tischhauser *et al.* [22] to fix the effective range parameters. The reported energies of the  $\alpha$  particle for the phase shift data in lab frame are  $T_\alpha \simeq 1.5$ -6.6 MeV and 2.6-6.6 MeV<sup>3</sup>, respectively, whereas, as mentioned above, we introduced the resonance energies as the large scales of the process. Thus we have the lowest momenta in the center of mass frame,  $k_{low} \simeq 80$  and 105 MeV for Ref. [21] and [22], respectively, whereas the highest momenta,  $k_{high} \simeq 166, 117$ , and 123 MeV for  $l = 0, 1$ , and 2 channels, respectively. Because the large momentum scale of the theory is  $\Lambda_H \sim 150$  MeV, though in the higher momentum region the series expansion would not converge, it may do in the relatively low momentum region. The convergence of the effective range expansion for each channel is to be studied below.

An effective Lagrangian for the present study may be written as [19, 23, 24]

$$\begin{aligned} \mathcal{L} = & \phi_\alpha^\dagger \left( iD_0 + \frac{\vec{D}^2}{2m_\alpha} + \dots \right) \phi_\alpha + \phi_C^\dagger \left( iD_0 + \frac{\vec{D}^2}{2m_C} + \dots \right) \phi_C \\ & + \sum_{l,n} C_n^{(l)} d_{(l)}^\dagger \left[ iD_0 + \frac{\vec{D}^2}{2(m_\alpha + m_C)} \right]^n d_{(l)} \\ & - \sum_l y_{(l)} \left[ (\phi_\alpha O_l \phi_C)^\dagger d_{(l)} + d_{(l)}^\dagger (\phi_\alpha O_l \phi_C) \right] + \dots, \end{aligned} \quad (1)$$

where  $\phi_\alpha$  ( $m_\alpha$ ) and  $\phi_C$  ( $m_C$ ) are point-like fields (masses) of  $\alpha$  and  $^{12}\text{C}$ , respectively.  $D_\mu$  is a covariant derivative, and the dots denote higher order terms.  $d_{(l)}$  represent  $\alpha$  and  $^{12}\text{C}$  composite fields of angular momentum  $l$ . Thus  $d_{(0)}$  for  $l = 0$ ,  $d_{(1)i}$  for  $l = 1$  where the subscript  $i$  represents a state in  $l = 1$ , and  $d_{(2)ij}$  for  $l = 2$  where  $d_{(2)ij} = d_{(2)ji}$  and the subscripts  $ij$  represent a state in  $l = 2$ .  $C_n^{(l)}$  are coupling constants for the propagation of the  $\alpha$ - $^{12}\text{C}$  composite fields for the  $l$  channels, and can be related to effective range parameters along with common multiplicative factors  $1/y_{(l)}^2$ . For the present exploratory study, three effective range parameters, the terms of  $n = 0, 1, 2$ , are retained for each partial wave. For the  $l = 0$  state, for example,  $C_0^{(0)}$  is related to the scattering length,  $C_1^{(0)}$  the effective range, and  $C_2^{(0)}$  the shape parameter. In addition,  $y_{(l)}$  are coupling constants of the  $\alpha$ - $^{12}\text{C}$ - $d_{(l)}$  vertices, and  $O_l$  are projection operators by which the  $\alpha$ - $^{12}\text{C}$  system is projected to the  $l$ -th partial wave states. Thus one has

$$O_0 = 1, \quad O_{1,i} = \frac{i \overleftrightarrow{D}_i}{M} \equiv i \left( \frac{\overrightarrow{D}_C}{m_C} - \frac{\overleftarrow{D}_\alpha}{m_\alpha} \right)_i, \quad O_{2,ij} = \frac{1}{M^2} \left( -\overleftrightarrow{D}_i \overleftrightarrow{D}_j + \frac{1}{3} \delta_{ij} \overleftrightarrow{D}^2 \right). \quad (2)$$

---

<sup>3</sup>The energies  $T_\alpha$  and  $T$  for the  $\alpha$ - $^{12}\text{C}$  system in lab and center of mass frames are related by  $T_\alpha \simeq \frac{4}{3}T$ .

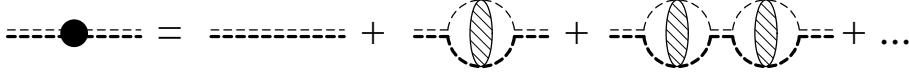


Figure 1: Diagrams for propagator of dressed composite fields. Double dashed line denotes bare composite ( $^{16}\text{O}$ ) field consisting of  $\alpha$  and  $^{12}\text{C}$  fields, thin (thick) dashed line denotes point-like  $\alpha$  ( $^{12}\text{C}$ ) field, and shaded blob denotes off-shell Coulomb T-matrix.

### 3. Scattering amplitudes and phase shifts

The differential cross section of the elastic  $\alpha$ - $^{12}\text{C}$  scattering (for two spin-0 charged particles) in terms of the phase shifts are given by (see, e.g., Ref. [25])

$$\begin{aligned} \sigma(\theta) &= \frac{d\sigma}{d\Omega} = |f(\theta)|^2 \\ &= \frac{1}{k^2} \left| -\frac{\eta}{2 \sin^2 \frac{1}{2}\theta} \exp\left(-2i\eta \ln \sin \frac{1}{2}\theta\right) \right. \\ &\quad \left. + \frac{1}{2} i \sum_{l=0}^{\infty} (2l+1) [\exp(2i\omega_l) - U_l] P_l(\cos \theta) \right|^2, \end{aligned} \quad (3)$$

where  $f(\theta)$  is the scattering amplitude including both pure Coulomb part and Coulomb modified strong interaction part,  $\theta$  is a scattering angle,  $k$  is the relative absolute momentum, and  $\eta = \kappa/k$ . In addition,  $\omega_l$  is the Coulomb scattering phase,  $\omega_l (= \sigma_l - \sigma_0) = \sum \arctan(\eta/s)$  for  $s = 1$  to  $l$ ,<sup>4</sup> and

$$U_l = \exp[2i(\delta_l + \omega_l)]. \quad (4)$$

$\delta_l$  are real scattering phase shifts.

The elastic scattering amplitudes for the Coulomb modified strong interaction part for  $l = 0, 1, 2$  channels are calculated from the effective Lagrangian presented above. In Fig. 1 Feynman diagrams for dressed composite  $^{16}\text{O}$  propagators consisting of the  $\alpha$  and  $^{12}\text{C}$  elementary-like fields including the Coulomb interaction between the two charged fields are depicted. In Fig. 2, a Feynman diagram for a scattering amplitude for elastic  $\alpha$ - $^{12}\text{C}$  scattering for each partial wave state including the initial and final state Coulomb interactions is depicted. For derivation of the amplitudes from the diagrams in detail the reader may refer to, e.g., Refs. [26, 27] and we do not repeat the detailed calculation.

Thus we have the scattering amplitudes,  $A_l$ , for  $l = 0, 1, 2$  states in terms of the effective range parameters as [19, 28]

$$A_0 = \frac{2\pi}{\mu - \gamma_0 + \frac{1}{2}r_0k^2 - \frac{1}{4}P_0k^4 - 2\kappa H(\eta)} \frac{C_\eta^2 e^{2i\sigma_0}}{\mu - \gamma_0 + \frac{1}{2}r_0k^2 - \frac{1}{4}P_0k^4 - 2\kappa H(\eta)}, \quad (5)$$

$$A_1 = \frac{6\pi}{\mu - \gamma_1 + \frac{1}{2}r_1k^2 - \frac{1}{4}P_1k^4 - 2\kappa k^2(1 + \eta^2)H(\eta)} \frac{e^{2i\sigma_1} k^2 (1 + \eta^2) C_\eta^2 \cos \theta}{\mu - \gamma_1 + \frac{1}{2}r_1k^2 - \frac{1}{4}P_1k^4 - 2\kappa k^2(1 + \eta^2)H(\eta)}, \quad (6)$$

<sup>4</sup> $\sigma_0$  is the Coulomb phase shift,  $\sigma_0 = \arg \Gamma(1 + i\eta)$ .

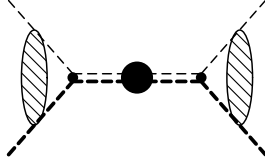


Figure 2: Diagram for scattering amplitudes. See the caption in Fig. 1 as well.

$$A_2 = \frac{10\pi}{\mu} \frac{e^{2i\sigma_2} k^4 (4 + \eta^2) (1 + \eta^2) C_\eta^2 \frac{1}{2} (3 \cos \theta - 1)}{-\gamma_2 + \frac{1}{2} r_2 k^2 - \frac{1}{4} P_2 k^4 - 2\kappa k^4 (4 + \eta^2) (1 + \eta^2) H(\eta)}, \quad (7)$$

with

$$C_\eta^2 = \frac{2\pi\eta}{e^{2\pi\eta} - 1}, \quad H(\eta) = \psi(i\eta) + \frac{1}{2i\eta} - \ln(i\eta), \quad (8)$$

where  $\psi(x)$  is the digamma function.  $\gamma_l$ ,  $r_l$ ,  $P_l$  are the three effective range parameters for  $l = 0, 1, 2$ . While the amplitudes,  $A_l$ , can be represented in terms of the phase shifts  $\delta_l$  as

$$A_0 = \frac{2\pi}{\mu} \frac{e^{2i\sigma_0}}{k \cot \delta_0 - ik}, \quad A_1 = \frac{6\pi}{\mu} \frac{e^{2i\sigma_1} \sin \theta}{k \cot \delta_1 - ik}, \quad A_2 = \frac{10\pi}{\mu} \frac{e^{2i\sigma_2} \frac{1}{2} (3 \cos \theta - 1)}{k \cot \delta_2 - ik}. \quad (9)$$

Thus one has the relations between the phase shifts and the effective range parameters as

$$C_\eta^2 k \cot \delta_0 + 2\kappa h(\eta) = -\gamma_0 + \frac{1}{2} r_0 k^2 - \frac{1}{4} P_0 k^4 + \dots, \quad (10)$$

$$k^2 (1 + \eta^2) \left[ C_\eta^2 k \cot \delta_1 + 2\kappa h(\eta) \right] = -\gamma_1 + \frac{1}{2} r_1 k^2 - \frac{1}{4} P_1 k^4 + \dots, \quad (11)$$

$$k^4 (4 + \eta^2) (1 + \eta^2) \left[ C_\eta^2 k \cot \delta_2 + 2\kappa h(\eta) \right] = -\gamma_2 + \frac{1}{2} r_2 k^2 - \frac{1}{4} P_2 k^4 + \dots, \quad (12)$$

where  $h(\eta) = \text{Re}H(\eta)$ .

#### 4. Fixing the parameters

Before fixing values of the effective range parameters, we discuss some features of the equations obtained in Eqs. (10,11,12). At low energies the function  $h(\eta)$  appearing in the equations can be expanded in terms of  $1/\eta (= k/\kappa)$  as

$$h(\eta) = \frac{1}{12\eta^2} + \frac{1}{120\eta^4} + \frac{1}{252\eta^6} + \dots \quad (13)$$

One may see that the series expansion converges in the energy region which we consider below and there is no constant term appearing from the  $h(\eta)$  function. In addition, the factor  $C_\eta^2$  being multiplied to the cotangent terms in Eqs. (10,11,12) becomes vanishingly small at the very low energies. Thus the left hand side of the equations vanishes in zero

	$S0$	$S1$	$S2$	$S3$
$\gamma_0$ (MeV)	$0.058 \pm 0.058$	$0.034 \pm 0.003$	$0.015 \pm 0.001$	$-0.008 \pm 0.001$
$r_0$ (fm)	$0.270 \pm 0.002$	$0.2693 \pm 0.0001$	$0.2685 \pm 0.0001$	$0.2674 \pm 0.0000$
$P_0$ (fm <sup>3</sup> )	$-0.037 \pm 0.005$	$-0.0372 \pm 0.0002$	$-0.0390 \pm 0.0001$	$-0.0416 \pm 0.0000$

Table 1: Fitted values of  $s$ -wave effective range parameters using four sets of the experimental data labeled by  $S0$ ,  $S1$ ,  $S2$ , and  $S3$ . See the text for details.

momentum limit,  $k \rightarrow 0$ , and the parameters  $\gamma_0$ ,  $\gamma_1$ , and  $\gamma_2$  in the right hand side of Eqs. (10), (11), and (12) are required to vanish as well in the limit. On the other hand, experimental data do not exist at such very low energies, and values of the parameters are fixed by using existing experimental data at some higher energies. As mentioned above, the experimental data from Plaga *et al.* [21] and Tischhauser *et al.*[22] where the lowest energies the data are  $T_\alpha \simeq 1.5$  and 2.6 MeV, respectively are employed up to the energies of the resonant states,  $T_\alpha \simeq 6.5$ , 3.2, and 3.6 MeV for  $l = 0, 1$ , and 2, respectively.<sup>5</sup>

We note that we have to choose  $\gamma_2 = 0$  in fitting the parameters because the phase shift for the  $l = 2$  channel is very small, less than two degrees, in the fitting energy range and it is not easy to have a non-vanishing contribution to  $\gamma_2$ . In addition, due to the feature in the zero momentum limit mentioned above, it is not easy to incorporate the pole structure of the subthreshold states in the amplitudes either because it makes the  $\gamma_l$  terms significantly large. Therefore, we fix the parameters, without including the pole structure of the subthreshold states, from data sets which we arbitrarily choose for each of the partial wave states,  $l = 0, 1, 2$ , below.

#### 4.1. $l = 0$ channel

Four sets of the experimental data for the  $s$ -wave phase shift are chosen in order to qualitatively study the dependence from the choice of the data sets for the extrapolation to  $T_G$ . The four sets of the data are labeled as  $S0$ ,  $S1$ ,  $S2$ , and  $S3$ .  $S0$  denotes a data set of the  $s$ -wave phase shift at energies  $T_\alpha = 1.5$ -6.5 MeV from Table 2 in the Plaga *et al.*'s paper [21], and  $S1$ ,  $S2$ , and  $S3$  do those at energies  $T_\alpha = 2.6$ -6.5, 2.6-6.0, and 2.6-5.0 MeV, respectively, from the Tischhauser *et al.*'s paper [22].

In Table 1 fitted values of the  $s$ -wave effective range parameters by using the four data sets,  $S0$ ,  $S1$ ,  $S2$ , and  $S3$  are displayed.<sup>6</sup> One can see that the fitted values of  $\gamma_0$  are sensitive to the choice of the data sets, those of  $r_0$  are not, and those of  $P_0$  are in between the two cases. We find that almost exact cancellations between the  $r_0$  term and the coefficient of the term proportional to  $k^2$ ,  $1/(3\kappa) \simeq 0.2687$  fm, from  $2\kappa h(\eta)$  term in Eq. (10) and significant cancellations between the  $P_0$  term and that of the term proportional to  $k^4$  term,  $-1/(15\kappa^3) \simeq -0.0210$  fm<sup>3</sup>, from the  $2\kappa h(\eta)$  term. As discussed

<sup>5</sup>Thus the momentum of the  $\alpha$ -<sup>12</sup>C system in the center of mass frame for the data becomes  $k = 80(105)$ -166 MeV for  $l = 0$ , 80(105)-117 MeV for  $l = 1$ , and 80(105)-123 MeV for  $l = 2$ .

<sup>6</sup>We employ a scipy module, `curve_fit`, in optimization package to fit the effective range parameters to the phase shift data.

in the introduction, we find that the expansion series in terms of the effective range parameters well converges in the energy regions for the fitting. Those coefficients of the  $k^{2n}$  power series after including the corrections from the  $2\kappa h(\eta)$  term become significantly small, e.g., the  $\gamma_0$  values being a few hundredth MeV, compared to the scale of the system. This may be due to the suppression factor from the  $C_\eta^2$  term in Eq. (10), which becomes  $C_\eta^2 \sim 10^{-6}$ - $10^{-4}$  in the range of the energy,  $T_\alpha \simeq 2.0$ - $6.0$  MeV.

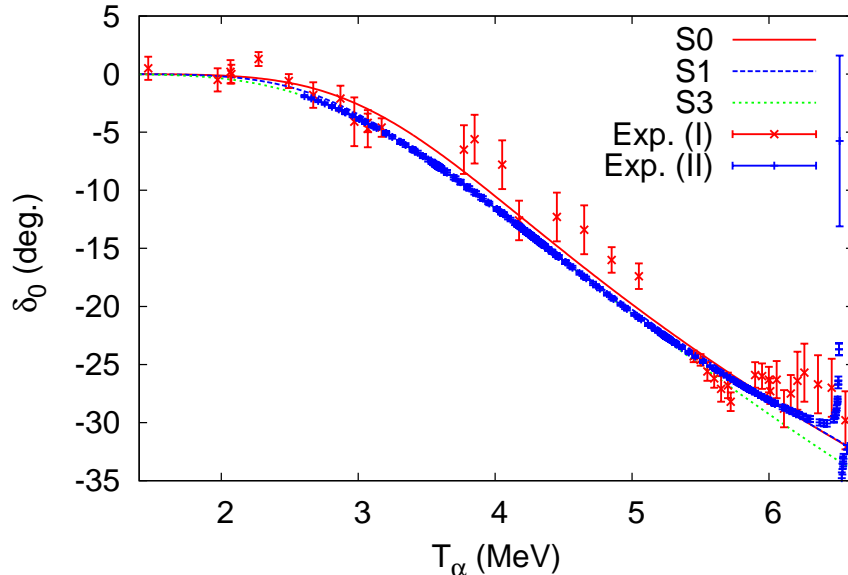


Figure 3: Phase shift of elastic  $\alpha$ - $^{12}\text{C}$  scattering for  $l = 0$ ,  $\delta_0$  (deg.), as functions of  $T_\alpha$  (MeV). Three curves are plotted by using three sets of fitted effective range parameters (labeled by  $S0$ ,  $S1$ ,  $S3$ ) obtained in Table 1. Experimental data labeled by Exp. (I) from Plaga *et al.* [21] and Exp. (II) from Tischhauser *et al.* [22] are also displayed.

In Fig. 3, curves of the  $s$ -wave phase shift are plotted by using the effective range parameters obtained in Table 1. The experimental data are also included in the figure. We find that the curves are well reproduced the data in the energy ranges where the effective range parameters have been fitted.

In Fig. 4, in order to qualitatively study the extrapolation to the Gamow energy,  $T_G = 0.3$  MeV in the center of mass frame, which corresponds to  $T_\alpha \simeq 0.4$  MeV in the lab frame, we plot curves of the real part of the denominator of the  $s$ -wave scattering amplitude in Eq. (5),

$$f_s(k) = -2\kappa h(\eta) - \gamma_0 + \frac{1}{2}r_0k^2 - \frac{1}{4}P_0k^4, \quad (14)$$

by using the values of the effective range parameters obtained in Table 1, as functions of  $T_\alpha$  where  $k = \sqrt{1.5\mu T_\alpha}$ . One can see that the fitted curves almost overlap at  $T_\alpha \simeq 3$ - $5$  MeV,

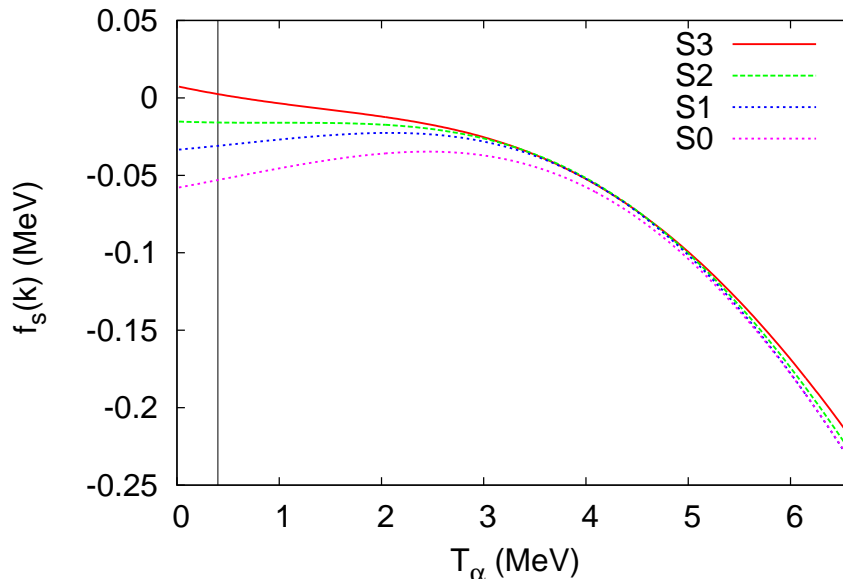


Figure 4: Function  $f_s(k)$  defined in Eq. (14) as functions of  $T_\alpha$  (MeV). Curves are plotted by using four sets of values of effective range parameters (labeled by  $S0$ ,  $S1$ ,  $S2$ ,  $S3$ ) obtained in Table 1. A vertical line at  $T_\alpha = 0.4$  MeV is also included.

except for the curve of  $S0$ , and when one extrapolates the curves to the lower energies, they are scattered. The curves of  $f_s(k)$  decreases, is almost the same, and increases at  $T_\alpha \simeq 0.4$  MeV, compared to the values of the function at  $T_\alpha \simeq 3$  MeV, depending on the choice of the data sets,  $S1$ ,  $S2$ , and  $S3$ , respectively. Thus we find a significant uncertainty in the extrapolation to the energy,  $T_\alpha \simeq 0.4$  MeV, corresponding to  $T_G$ . We note that the curve of  $S3$  vanishes at a small value of  $T_\alpha$ . That indicates the presence of the resonant state at the very low energy and thus the parameter set  $S3$  should be excluded.

#### 4.2. $l = 1$ channel

Three sets of the experimental data for the  $p$ -wave phase shift to fit the effective range parameters are chosen, and labeled as  $P0$ ,  $P1$ , and  $P2$ .  $P0$  denotes a data set of the  $p$ -wave phase shift at  $T_\alpha \simeq 1.5$ -3.1 MeV from Table 2 in the Plaga *et al.*'s paper [21], and  $P1$  and  $P2$  do those at  $T_\alpha = 2.6$ -3.0 MeV and 2.6-3.1 MeV, respectively, from the Tischhauser *et al.*'s paper [22]. We note that, as mentioned above, we chose the largest energies of the data sets less than the resonance energy,  $T_\alpha \simeq 3.23$  MeV.

In Table 2 fitted values of the  $p$ -wave effective range parameters by using the three sets of the data labeled by  $P0$ ,  $P1$ , and  $P2$  are displayed. We find in Table 2 the similar tendency to what we found in the fitted values of the  $s$ -wave effective range parameters in Table 1. The fitted values of  $\gamma_1$  are quite sensitive to the choice of the data sets, whereas those of  $r_1$  and  $P_1$  do not. We can see that the significant cancellations between the  $r_1$

	$P0$	$P1$	$P2$
$\gamma_1$ ( $10^3$ MeV <sup>3</sup> )	$-2.53 \pm 1.09$	$-3.84 \pm 1.27$	$-4.57 \pm 0.38$
$r_1$ (fm <sup>-1</sup> )	$0.406 \pm 0.002$	$0.405 \pm 0.002$	$0.404 \pm 0.000$
$P_1$ (fm)	$-0.641 \pm 0.006$	$-0.645 \pm 0.007$	$-0.649 \pm 0.002$

Table 2: Fitted values of  $p$ -wave effective range parameters using three sets of the experimental data labeled by  $P0$ ,  $P1$ , and  $P2$ . See the text for details.

( $P_1$ ) term and the term proportional to  $k^2$  ( $k^4$ ) obtained from the  $2\kappa k^2(1 + \eta^2)h(\eta)$  term in Eq. (11) where we have  $\frac{1}{3}\kappa \simeq 0.413$  fm<sup>-1</sup> corresponding to the  $r_1$  term and  $-11/15\kappa \simeq -0.591$  fm corresponding to the  $P_1$  term. We also find that the series expansion of the effective range parameters converges at very low energies, up to about  $T_\alpha \simeq 1.5$  MeV, and the significant cancellations occur between the terms being proportional to  $k^2$  and  $k^4$  in the energy range,  $T_\alpha \simeq 2$ -3 MeV.

In Fig. 5, curves of the phase shift of the elastic  $p$ -wave  $\alpha$ -<sup>12</sup>C scattering are plotted by using the fitted effective range parameters in Table 2. The experimental data are also included in the figure. We find that the curves well reproduce the data in the energy ranges where the effective range parameters have been fitted.

In Fig. 6 we plot the real part of the denominator of the  $p$ -wave scattering amplitude in Eq. (6),

$$f_p(k) = -2\kappa k^2(1 + \eta^2)h(\eta) - \gamma_1 + \frac{1}{2}r_1 k^2 - \frac{1}{4}P_1 k^4, \quad (15)$$

by using the values of the effective range parameters obtained in Table 2 as functions of  $T_\alpha$ . One can see that the values of the function  $f_p(k)$  are small at the energy range,  $T_\alpha = 2.6$ -3.0 MeV. In that energy region, as mentioned above, a significant cancelation among the terms of the effective range expansion occurs. While the values of the  $f_p(k)$  function become large when it is extrapolated to  $T_\alpha = 0.4$  MeV, due to the relatively large contribution from the  $\gamma_1$  term compared to the other effective range terms of  $r_1$  and  $P_1$  when the corrections from the  $2\kappa k^2(1 + \eta^2)h(\eta)$  term are included. This implies that because the function  $f_p(k)$  appears in the denominator of the scattering amplitude the scattering amplitude is rather suppressed at  $T_G$ . Thus we cannot qualitatively reproduce the enhancement of the  $S$ -factor for the E1 channel, reported, e.g., in Ref. [29], in the extrapolation of the  $p$ -wave scattering amplitude to  $T_G$ .

### 4.3. $l = 2$ channel

Three sets of the experimental data for the  $d$ -wave phase shift to fit the effective range parameters are chosen, and labeled as  $D0$ ,  $D1$ , and  $D2$ .  $D0$  denotes a data set of the  $d$ -wave phase shift at  $T_\alpha \simeq 1.47$ -3.57 MeV from Table 2 in the Plaga *et al.*'s paper [21], and  $D1$  and  $D2$  do those at  $T_\alpha = 2.6$ -3.0 and 2.6-3.4 MeV, respectively, from the Tischhauser *et al.*'s paper [22]. We note that the maximum energies of the data sets are chosen as less than the resonance energy,  $T_\alpha \simeq 3.57$  MeV.

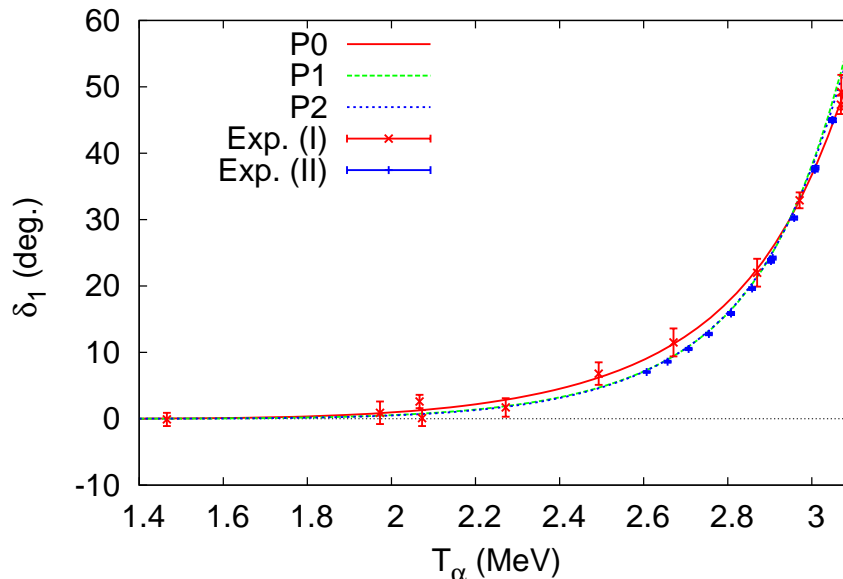


Figure 5: Phase shift of elastic  $\alpha$ - $^{12}\text{C}$  scattering for  $l = 1$ ,  $\delta_1$  (deg.), as functions of  $T_\alpha$  (MeV). Three curves are plotted by using three sets of fitted effective range parameters (labeled by  $P0$ ,  $P1$ ,  $P2$ ) obtained in Table 2. Experimental data, Exp. (I) from Plaga *et al.* [21] and Exp. (II) from Tischhauser *et al.* [22], are also displayed.

In Table 3 fitted values of the  $d$ -wave effective range parameters by using the three data sets introduced above are displayed. As mentioned before we have chosen  $\gamma_2 = 0$  due to the small values of the phase shift in those data sets. We find that large error bars of the fitted parameters from the data set  $D0$  compared to those from the data sets,  $D1$  and  $D2$ . We also find the common tendency that the significant cancellations between the  $r_2$  ( $P_2$ ) term and the term proportional to  $k^2$  ( $k^4$ ) obtained from the  $2\kappa k^4(4+\eta^2)(1+\eta^2)h(\eta)$  term in Eq. (12) where we have  $\frac{1}{3}\kappa^3 \simeq 0.6361 \text{ fm}^{-3}$  and  $-\frac{51}{15}\kappa \simeq -4.217 \text{ fm}^{-1}$  corresponding to  $r_2$  and  $P_2$ , respectively. For the convergence of the effective range expansion, we find that there is no convergence for the terms. There are large cancellations between the terms proportional to  $k^2$  and  $k^4$  at the energies  $T_\alpha \simeq 1.5\text{-}2 \text{ MeV}$ . At the larger energies, the  $k^4$  term becomes dominant and is significantly cancelled with the other terms.

In Fig. 7, curves of the  $d$ -wave phase shift are plotted by using the fitted values of the effective range parameters obtained in Table 3. The experimental data are also included in the figure. We can see that the curves plotted in the figure well reproduce the experimental data in the energy range below the resonance energy,  $T_\alpha \simeq 3.57 \text{ MeV}$ , and the error bars of the Tischhauser *et al.*'s data are significantly smaller than those of the Plaga *et al.*'s data.

In Fig. 8 we plot curves of the real part of the denominator of the  $d$ -wave scattering

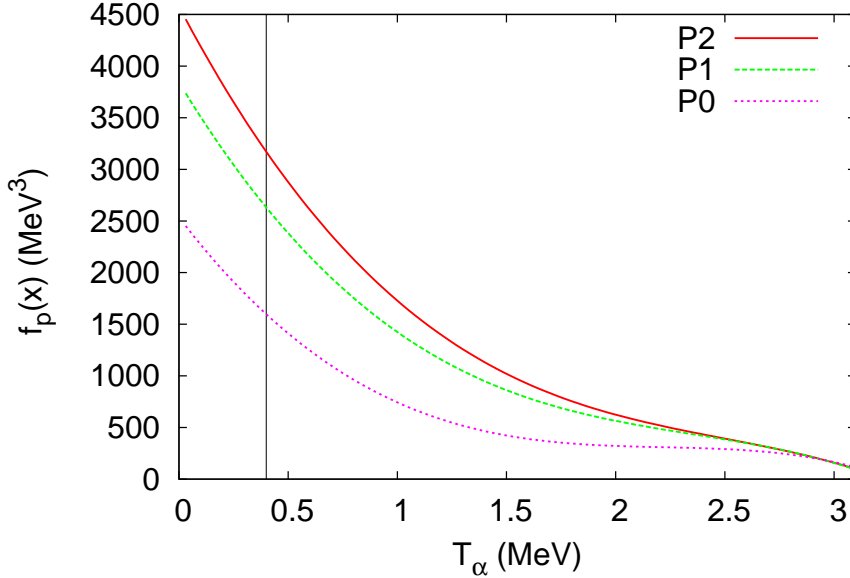


Figure 6: Function  $f_p(k)$  defined in Eq. (15) as functions of  $T_\alpha$  (MeV). Curves are plotted by using three sets of values of effective range parameters (labeled by  $P0$ ,  $P1$ ,  $P2$ ) obtained in Table 2. A vertical line at  $T_\alpha = 0.4$  MeV is also included.

amplitude in Eq. (7),

$$f_d(k) = -2\kappa k^4(4 + \eta^2)(1 + \eta^2)h(\eta) - \gamma_2 + \frac{1}{2}r_2k^2 - \frac{1}{4}P_2k^4, \quad (16)$$

by using the values of the effective range parameters in Table 3 as functions of  $T_\alpha$ . One can see that the curves vanish in the limit where  $k \rightarrow 0$  because of the assumption of  $\gamma_2 = 0$ . In addition, the tracks of the extrapolation for the data sets of  $D1$  and  $D2$  are quite different from that of  $D0$ , whereas as mentioned before, the curve from the  $D0$  data set should have a large uncertainty due to the large error bars of the fitted parameters. Furthermore, we find that the curves of  $D1$  and  $D2$  are almost flat from  $T_\alpha \simeq 2$  MeV to  $T_\alpha \simeq 0.4$  MeV, so the extrapolated cross section would be almost the same except for the common factor  $C_\eta^2$  at  $T_G$  and  $T \simeq 2$  MeV. Thus we cannot qualitatively reproduce the enhancement of the  $S$ -factor for the E2 channel either, reported, e.g., in Ref. [30], in the extrapolation of the  $d$ -wave scattering amplitude to  $T_G$ .

## 5. Discussion and conclusions

In this work we introduce an EFT for the  $^{12}\text{C}(\alpha, \gamma)^{16}\text{O}$  at  $T_G$  where the  $\alpha$  and  $^{12}\text{C}$  states are treated as the elementary-like cluster fields, and apply the theory to the study of the phase shifts of the elastic  $\alpha$ - $^{12}\text{C}$  scattering for  $l = 0, 1, 2$  channels at the low energies. The expression of the scattering amplitudes for  $l = 0, 1, 2$  channels is obtained in terms of

	<i>D0</i>	<i>D1</i>	<i>D2</i>
$r_2$ (fm <sup>-3</sup> )	$0.37 \pm 0.79$	$0.536 \pm 0.001$	$0.533 \pm 0.001$
$P_2$ (fm <sup>-1</sup> )	$-6.2 \pm 4.3$	$-5.505 \pm 0.008$	$-5.526 \pm 0.004$

Table 3: Fitted values of *d*-wave effective range parameters using three sets of the experimental data labeled by *D0*, *D1*, and *D2*. See the text for details.

the three effective range parameters. The effective range parameters are fitted by using the sets of the experimental data in the energy ranges below the resonance energies in which the phase shifts are smoothly varying. In the parameter fitting we find that it is difficult to incorporate the pole structure for the subthreshold  $1_1^-$  and  $2_1^+$  states in the amplitudes. Nevertheless we find that the experimental data at the low energies are well reproduced by the curves plotted using the fitted effective range parameters. To qualitatively study the uncertainty of the extrapolation to  $T_G$  due to the fitting of the parameters to the experimental phase shift data, we extrapolate the real part of the denominator of the scattering amplitudes to  $T_G$ , and find that there are the significant uncertainties. Because parameters deduced from the scattering phase shifts for  $l = 1$  and 2 channels may play important roles in the extrapolation of the *S*-factors of the radiative capture reaction for the E1 and E2 transitions, we discuss our results in the parameter fitting and the extrapolation of the scattering amplitudes to  $T_G$  in some details below.

In the parameter fitting for the  $l = 1$  channel, the phase shift data entirely appear as the low energy tail of the  $1_2^-$  resonant state, and the tail from the  $1_1^-$  bound state at  $T = -0.045$  MeV can be scarcely seen in the data. As we have found above, to reproduce the data it is not necessary to include the subthreshold bound state. In addition, the amplitude extrapolated to  $T_G$  is largely suppressed. Those observations in fact have repeatedly been pointed out in the literatures [31, 32, 33]. Indeed, to estimate the radiative capture *E1* transition cross section at  $T_G$ , it would be essential to include an explicit degree of freedom for the  $1_1^-$  state in the theory, possibly along with the  $1_2^-$  state [34]. Although the tail of the the  $1_1^-$  state is not clearly seen in the elastic scattering data, the significance of the  $1_1^-$  bound state may be seen in the other experimental data such as the  $\beta$ -delayed  $\alpha$  decay from  $^{16}\text{N}$ ,  $^{16}\text{N}(\beta^-)^{16}\text{O}(\alpha)^{12}\text{C}$  [35, 36, 37], whose minimum energy is  $T = 0.6$  MeV, and the radiative *E1* capture cross section whose minimum energy now becomes less than  $T = 1$  MeV, see, e.g., Refs. [38, 39, 40].

In the parameter fitting for the  $l = 2$  channel, the phase shift data at  $T_\alpha = 1.5$ - $3.5$  MeV show a down slope up to the  $2_2^+$  resonant state appearing at  $T_\alpha = 3.57$  MeV. As demonstrated above, it is not difficult to fit the restricted data by using the three effective range parameters, but it appears not easy to precisely decompose it into three ingredients, the tail of the subthreshold state, that of the resonant state, and a background. Moreover, as discussed, it is not easy to include the  $2_1^+$  subthreshold state at  $T = -0.24$  MeV because of the feature of the scattering amplitudes (represented in terms of the effective range parameters) in the present study. In the extrapolation, as seen above, we find that almost

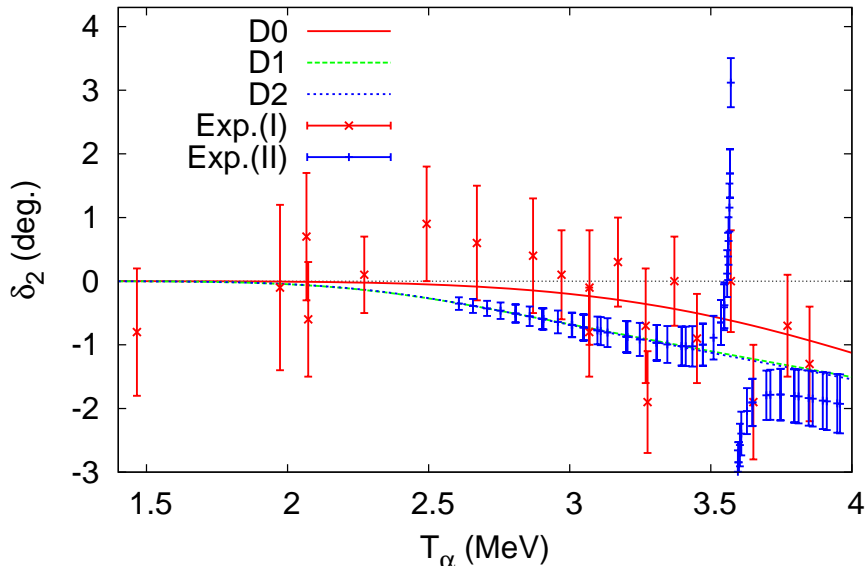


Figure 7: Phase shift of elastic  $\alpha$ - $^{12}\text{C}$  scattering for  $l = 2$ ,  $\delta_2$  (deg.), as functions of  $T_\alpha$  (MeV). Three curves are plotted by using three sets of fitted effective range parameters (labeled by  $D0$ ,  $D1$ ,  $D2$ ) obtained in Table 3. Experimental data, Exp. (I) from Plaga *et al.* [21] and Exp. (II) from Tischhauser *et al.* [22], are also displayed.

the similar magnitude of the denominator of the scatter amplitude at  $T_G$  and  $T_\alpha \simeq 2$  MeV. This observation can be questionable because the series of the effective range expansion we obtained does not converge. Thus to extrapolate the radiative  $E2$  capture cross section to  $T_G$  in the present theory, it would be essential to include an explicit degree of freedom for the subthreshold  $2_1^+$  state as well. Moreover, as pointed out by Sparenberg [41], asymptotic normalization constant (ANC) for the  $2_1^+$  state is not possible to determine from single channel scattering phase shift data, it may be necessary to fix couplings for the  $2_1^+$  state from model calculations, such as a supersymmetric potential model assuming rotational band for the  $0_2^+$ ,  $2_1^+$ ,  $4_1^+$ , and  $6_1^+$  states for  $^{16}\text{O}$  [41], or a microscopic cluster model [42]. It may also be possible to estimate the parameters from other experimental data, such as a cascade transition to the  $2_1^+$  state [43, 44] or  $\gamma$  distribution of the radiative capture rate at the very low energies [38, 39, 40].

### Acknowledgements

The author would like to thank K. Kubodera for encouragement to the present work and S.-W. Hong and T.-S. Park for discussions. This work is supported by the Sunmoon University Research Grant of 2015.

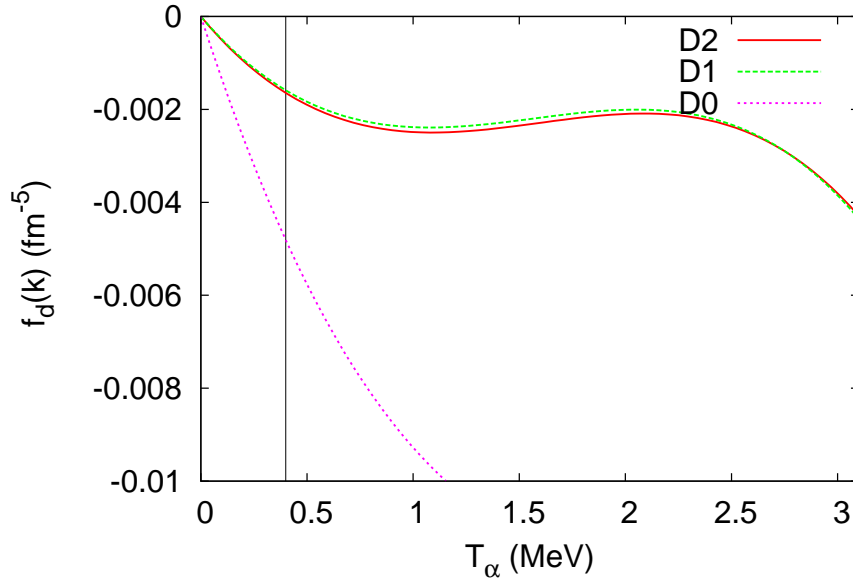


Figure 8: Function  $f_d(k)$  defined in Eq. (16) as functions of  $T_\alpha$  (MeV). Curves are plotted by using three sets of values of effective range parameters (labeled by  $D0$ ,  $D1$ ,  $D2$ ) obtained in Table 3. A vertical line at  $T_\alpha = 0.4$  MeV is also included.

## References

- [1] W. A. Fowler, Rev. Mod. Phys. 56, 149 (1984).
- [2] L. R. Buchmann and C. A. Barnes, Nucl. Phys. A 777, 254 (2006).
- [3] A. Coc, F. Hammache, and J. Kiener, Eur. Phys. J. A 51, 34 (2015).
- [4] Y. Xu *et al.*, Nucl. Phys. A 918, 61 (2013).
- [5] M. Gai, J. Phys. G 24, 1625 (1998).
- [6] M. Gai, Phys. Rev. C 88, 062801(R) (2013).
- [7] P.F. Bedaque and U. van Kolck, Ann. Rev. Nucl. Part. Sci. 52, 339 (2002).
- [8] E. Braaten and H.-W. Hammer, Phys. Rept. 428, 259 (2006).
- [9] U.-G. Meißner, arXiv:1510.03230.
- [10] G. Rupak, Nucl. Phys. A 678, 405 (2000).
- [11] S. Ando, R.H. Cyburt, S.W. Hong, and C.H. Hyun, Phys. Rev. C 74, 025809 (2006).

- [12] X. Kong and F. Ravndal, Nucl. Phys. A 656, 421 (1999).
- [13] M. Butler and J.-W. Chen, Phys. Lett. B 520, 87 (2001).
- [14] S. Ando, J.W. Shin, C.H. Hyun, S.W. Hong, and K. Kubodera, Phys. Lett. B 668, 187 (2008).
- [15] J.-W. Chen, C.-P. Liu, and S.-H. Yu, Phys. Lett. B 720, 385 (2013).
- [16] X. Zhang, K.M. Nollett, and D.R. Phillips, Phys. Rev. C 89, 051602(R) (2014).
- [17] E. Ryberg, C. Forssen, H.-W. Hammer, L. Platter, Eur. Phys. J. A 50, 170 (2014).
- [18] T. Teichmann, Phys. Rev. 83, 141 (1951).
- [19] R. Higa, H.-W. Hammer, and U. van Kolck, Nucl. Phys. A 809, 171 (2008).
- [20] S.-I. Ando and Y. Oh, Phys. Rev. C 90, 037301 (2014).
- [21] R. Plaga *et al.*, Nucl. Phys. A 465 (1987) 291-316.
- [22] P. Tischhauser *et al.*, Phys. Rev. C 79, 055803 (2009).
- [23] P.F. Bedaque, H.-W. Hammer, U. van Kolck, Phys. Lett. B 569 (2003) 159-167.
- [24] S. Ando and C.H. Hyun, Phys. Rev. C 72, 014008 (2005).
- [25] A.M. Lane, Rev. Mod. Phys. 30, 257 (1957).
- [26] S. Ando, J.W. Shin, C.-H. Hyun, and S.W. Hong, Phys. Rev. C 76, 064001 (2007).
- [27] S. Ando, Eur. Phys. J. A 33, 185 (2007).
- [28] R. Higa, EPJ Web. Conf. 3, 06001 (2010).
- [29] S.E. Koonin, T.A. Tombrello, G. Fox, Nucl. Phys. A 220, 221 (1974).
- [30] K. Langanke and S.E. Koonin, Nucl. Phys. A 410, 334 (1983).
- [31] G.M. Hale, Nucl. Phys. A 621, 177c (1997).
- [32] J. Humblet, Nucl. Phys. A 688, 552c (2001).
- [33] P. Descouvemont, M. Dufour, and J.-M. Sparenberg, Phys. Rev. C 81, 029803 (2010).
- [34] B.A. Gelman, Phys. Rev. C 80, 034005 (2009).
- [35] H. Hatting, K. Hunchen, and H. Waffler, Phys. Rev. Lett. 25, 941 (1970).
- [36] L. Buchmann *et al.*, Phys. Rev. Lett. 70, 726 (1993).

- [37] X.D. Tang *et al.*, Phys. Rev. C 81, 045809 (2010).
- [38] G. Roters *et al.*, Eur. Phys. J. A 6, 451 (1999).
- [39] M. Assuncao *et al.*, Phys. Rev. C 73, 055801 (2006).
- [40] R. Plag *et al.*, Phys. Rev. C 86, 015805 (2012).
- [41] J.-M. Sparenberg, Phys. Rev. C 69, 034601 (2004).
- [42] M. Dufour and P. Descouvemont, Phys. Rev. C 78, 015808 (2008).
- [43] L. Buchmann, Phys. Rev. C 64, 022801(R) (2001).
- [44] F.C. Barker and T. Kajino, Aust. J. Phys. 44, 369 (1991).